Development/Plasticity/Repair

Opposing Action of Nuclear Factor κB and Polo-like Kinases Determines a Homeostatic End Point for Excitatory Synaptic Adaptation

Anca B. Mihalas,[1] Yoichi Araki,[2] Richard L. Huganir,[1,2] and Mollie K. Meffert[1,2]

[1]Department of Biological Chemistry and [2]Solomon H. Snyder Department of Neuroscience, School of Medicine, Johns Hopkins University, Baltimore, Maryland 21205

Homeostatic responses critically adjust synaptic strengths to maintain stability in neuronal networks. Compensatory adaptations to prolonged excitation include induction of Polo-like kinases (Plks) and degradation of spine-associated Rap GTPase-activating protein (SPAR) to reduce synaptic excitation, but mechanisms that limit overshooting and allow refinement of homeostatic adjustments remain poorly understood. We report that Plks produce canonical pathway-mediated activation of the nuclear factor κB (NF-κB) transcription factor in a process that requires the kinase activity of Plks. Chronic elevated activity, which induces Plk expression, also produces Plk-dependent activation of NF-κB. Deficiency of NF-κB, in the context of exogenous Plk2 expression or chronic elevated neuronal excitation, produces exaggerated homeostatic reductions in the size and density of dendritic spines, synaptic AMPA glutamate receptor levels, and excitatory synaptic currents. During the homeostatic response to chronic elevated activity, NF-κB activation by Plks subsequently opposes Plk-mediated SPAR degradation by transcriptionally upregulating SPAR in mouse hippocampal neurons *in vitro* and *in vivo*. Exogenous SPAR expression can rescue the overshooting of homeostatic reductions at excitatory synapses in NF-κB-deficient neurons responding to elevated activity. Our data establish an integral feedback loop involving NF-κB, Plks, and SPAR that regulates the end point of homeostatic synaptic adaptation to elevated activity and are the first to implicate a transcription factor in the regulation of homeostatic synaptic responses.

Introduction

Homeostatic plasticity is an adaptive mechanism in which neurons sense their activity and respond to maintain it within a relatively constant optimum range. Synapse remodeling is a dynamic component of this adaptive response involving structural and functional modification of synapses, as well as synapse elimination or addition. Multiple molecular mechanisms, operating over different time scales, have been demonstrated to participate in homeostatic synaptic remodeling. However, several key elements of homeostatic adaptation, including factors that prevent the overshooting of responses and mechanisms determining the equilibrium end point of synaptic responses, remain incompletely defined (Turrigiano, 2008).

Received May 20, 2013; revised Aug. 20, 2013; accepted Sept. 6, 2013.

Author contributions: A.B.M., R.L.H., and M.K.M. designed research; A.B.M., Y.A., and M.K.M. performed research; A.B.M. and M.K.M. analyzed data; A.B.M. and M.K.M. wrote the paper.

This work was supported by National Institute of Mental Health Grant MH080740 (M.K.M.), National Institutes of Neurological Disorders and Stroke Grants NS36715 (R.L.H.) and MH084020 (to the Neuroscience Multiphoton Facility), American Cancer Society Research Scholar Grant 117028-RSG-09-056-01-GMC, and the Braude Foundation (M.K.M.). We thank M. Kaileh for the ChIP protocol and R. Sen for expert assistance with ChIP experiments, M. Pasparakis for the *RelA*$^{F/F}$ mouse line, M. Boersma and M. Riccomagno for plasmid construction, and J. Pomerantz and the Meffert laboratory for scientific suggestions and critical reading of this manuscript.

The authors declare no competing financial interests.

A. B. Mihalas's present address: Seattle Children's Research Institute, Center for Integrative Brain Research, Seattle, WA 98101.

Correspondence should be addressed to Mollie K. Meffert, School of Medicine, Johns Hopkins University, 725 N Wolfe Street, Baltimore, MD 21205. E-mail: mkm@jhmi.edu.

DOI:10.1523/JNEUROSCI.2131-13.2013

 0270-6474/13/3316490-12$15.00/0

Homeostatic plasticity at central glutamatergic synapses is evoked in response to prolonged changes in network activity (O'Brien et al., 1998; Turrigiano et al., 1998; Burrone et al., 2002) and can occur during development, learning, and injury repair. Polo-like kinases (Plks) are a family of cell cycle-associated serine/threonine kinases that are co-opted in the brain to function in stabilizing changes in synaptic strength during homeostatic responses to prolonged activity. Plk2 and Plk3 family members are activity inducible and targeted to dendritic spines (Kauselmann et al., 1999; Pak and Sheng, 2003), where they promote synapse dismantling and downregulate neuronal activity (Pak and Sheng, 2003; Seeburg and Sheng, 2008; Seeburg et al., 2008) through phosphorylating proteins, including the postsynaptic spine-associated Rap GTPase-activating protein (SPAR; Pak and Sheng, 2003). Phosphorylation of SPAR leads to its degradation, which enhances overall Rap relative to opposing Ras activity, and promotes actin reorganization and dendritic spine loss, AMPAR internalization, and a depression of synaptic strength (Pak et al., 2001; Zhu et al., 2002, 2005; Pak and Sheng, 2003; Lee et al., 2011).

The nuclear factor κB (NF-κB) family of transcription factors has been shown to be required for memory formation and recall in a variety of learning paradigms in both invertebrate and mammalian systems (Freudenthal and Romano, 2000; Meffert et al., 2003; Kaltschmidt et al., 2006; O'Riordan et al., 2006; Ahn et al., 2008). Previous work indicates that neuronal NF-κB promotes excitatory synaptic function in the mammalian CNS, which could underlie its role in learning and memory. NF-κB enhances

the size and density of dendritic spines and excitatory synapses during development and in response to plasticity, as well as enhancing excitatory synaptic currents (Boersma et al., 2011). Interestingly, a previous expression-cloning screen in heterologous cells identified Plk2 as a potent activator of NF-κB (Pomerantz et al., 2002). Our confirmation of this finding in primary murine hippocampal neurons suggested the possibility of an integral feedback loop involving NF-κB and Plks that might regulate synaptic responses during homeostatic plasticity. We found that neuronal Plks, which are expressed in response to elevated excitatory transmission, also activate NF-κB. NF-κB activation opposes and limits the dendritic spine loss and the reduction of excitatory synaptic responses mediated by Plk2. Collectively, the opposing forces of NF-κB and Plks provide positive and negative feedback to determine neuronal levels of SPAR and establish a homeostatic control system to stabilize and govern the equilibrium end point of homeostatic synaptic adaptation to sustained neuronal excitation.

Materials and Methods

Expression constructs and lentivirus preparation. GFP-Plk2 was constructed by subcloning murine Plk2 coding region (Open Biosystems, clone MGC: 7061) into the eGFP-C1 vector (Clontech); kinase-active and kinase-dead Plk2 were made by mutation of T236E and K108M, respectively. GFP-Plk2, GFP-Plk2 T236E, and Myr-GFP-F2A-p65 (M. Boersma, Harvard, Cambridge, MA) were also subcloned into the flap-ubiquitin-promoter-woodchuck regulatory element (FUW) lentiviral vector. pCMV-PSD95-eBFP2 was constructed by subcloning eBFP2 into pCMV-PSD95-eGFP (gift from R. Huganir, Johns Hopkins, Baltimore, MD). The following constructs were gifts: Plk3 wild-type (wt) and kinase-dead Plk3^{K91R} (P. Chiao, University of Texas, Austin, TX; Li et al., 2005); pCAG-Cre-IRES-DsRed (M. Riccomagno, and A. Kolodkin, Johns Hopkins, Baltimore, MD), mCherry (R. Tsien, University of California San Diego, San Diego, CA). pCMV-GFP-p65, FU-GFP-F2A-CreER^{T2}–WRE (CreER^{T2} coupled to expression of equivalent levels of eGFP by an F2A sequence), and lentiviral preparation were previously described (Boersma et al., 2011). pCMV-Luc-SPAR was constructed by N-terminal fusion of the murine SPAR coding region (Open Biosystems, clone MGC:106311) to luciferase-2 (Promega pGL4.10[luc2]) and insertion to pCMV-C1 (Clontech). Luciferase reporter for SPAR promoter activity was constructed by PCR amplification of *SIPA1L1* promoter (−508 to +688 bp around the predicted transcriptional start site) from mouse hippocampal tissue (PCR assembly of three adjacent fragments, about 400 bp each, that were individually PCR amplified) and insertion into Promega pGL4.12[luc2CP] vector, which lacks promoter and enhancer elements.

Hippocampal cultures and in vivo *analysis.* All mice were maintained in a temperature- and humidity-controlled facility on a 12 h light/dark cycle with food and water *ad libitum*. Animal care and experimental procedures were approved by the animal care committee of the Johns Hopkins University according to NIH guidelines. Dissociated hippocampal cultures from wild-type (ICR) or *RelA$^{F/F}$* mice (males and females) were prepared and subjected to lentiviral CreER^{T2}-mediated recombination as described previously (Boersma et al., 2011) by delivery of 4-hydroxy tamoxifen (OHT) 2.5 d before use, or transfected with pCAG-Cre-IRES-dsRed for 48 h when required. Murine hippocampi were dissociated and cells plated at a density of 200,000 cells/cm^2 on glass-bottom dishes (MatTek) for confocal imaging experiments, or 260,000 cells/cm^2 for immunoblotting experiments. Transfections were performed using lipofectamine 2000 (Invitrogen) according to the manufacturer's protocol. Picrotoxin (Sigma P1675; 100 μM, 24 h) was used to elicit homeostatic neuronal responses; interaction of the magnitude and the duration of stimuli, as well as culture conditions, influence the occurrence of potentiating or homeostatic responses to enhanced excitation (for review, see Nimchinsky et al., 2002). Homeostatic responses have been similarly observed by $GABA_A$ receptor inhibition using 20 μM bicuculline for 48 h (Turrigiano et al., 1998) or 100 μM picrotoxin for 24 h (Sun and Turrigiano, 2011). In contrast, enhanced synaptic response and spine density can be observed with exposure to low dose excitation [e.g., 10 μM picrotoxin (PTX), 24 h (Papa and Segal, 1996), or 25 μM bicuculline, 24 h (Boersma et al., 2011)], which can induce brief NF-κB activation that is calcium dependent and not Plk dependent (Meffert et al., 2003).

In vivo analysis was conducted from hippocampus after injection of adeno-associated virus (AAV) (AAV2/9.CMV.HII.GFP-Cre.WPRE.SV40, AAV2/9.CMV.PI.EGFP.WPRE.bGH; Penn Vector Core) in postnatal day 0 (P0) mouse pups, as described previously (Passini and Wolfe, 2001). *In vivo* analysis of SPAR dependence on NF-κB was conducted in *RelA$^{F/F}$* mice that were transduced with GFP or GFP-Cre recombinase by P0 injections of 2 μl AAV into each lateral ventricle. Eleven to 13 d after infection, each hippocampus was either harvested separately in lysis buffer and proteins resolved by SDS-PAGE or, for histochemical analysis of infection efficiency, hippocampi were fixed for 4 h at 4°C in PBS containing 4% paraformaldehyde and 4% sucrose, followed by 30% sucrose overnight incubation at 4°C. Hippocampi were then frozen in embedding media (OCT, Tissue-Tek 4583) and cryosectioned, with nuclei counterstained using Hoechst 33258 (Sigma B2883, 1 μg/ml, in 1% BSA, 0.1% Triton X-100 PBS), and mounted in 2.5% 1,4-diazabicyclo[2,2,2]octane solution (DABCO) (Sigma, catalog #D2522) and Fluoromount G (Cell Lab, catalog #731604).

Immunocytochemistry and immunoblotting. Immunocytochemistry and immunoblotting were performed as described previously (Lin et al., 2009; Boersma et al., 2011). Hippocampal neurons cultured on glass-bottom dishes (MatTek) were transfected with 15 ng pCMV-PSD95-eBFP2, 300 ng pCAG-Cre-IRES-dsRed, or 10 ng mCherry and empty vector pcDNA3.1 up to a total of 350 ng DNA and left to express for 48 h. At DIV21, they were subjected to brief live staining (10°C incubation for 15 min in ACSF 1.5% BSA; Lin et al., 2009) with N-terminus mouse ascites anti-GluA1 (gift from R. Huganir). Then, they were fixed in 4% paraformaldehyde 4% sucrose, permeabilized in 0.2% Triton X-100, and blocked in 10% BSA. Neurons were then incubated in 3% BSA with primary antibodies, chicken anti-GFP (Aves) and rabbit anti-dsRed (Clontech; catalog #632496), and secondary antibodies, anti-mouse Alexa 488, anti-rabbit Alexa 568, and anti-chicken Alexa 633 (Invitrogen), followed by mounting in 0.1 M *n*-propyl gallate in 50% glycerol.

Primary hippocampal cultures were lysed in buffer containing 50 mM HEPES, 150 mM NaCl, 1 mM EDTA, 10% glycerol, 1% Triton X-100, and 0.2% SDS, pH 7.9. Equal protein amounts (measured by Bradford assay, Bio-Rad) were loaded onto SDS-PAGE gels and transferred to PVDF membrane. Membranes were blocked in 5% milk TBST and subjected to primary antibodies: mouse anti-GluA1 (Millipore; ab-1504), mouse anti-β-actin (Developmental Studies Hybridoma Bank; JLA20), mouse anti-GABA(A)R, Alpha1 (NeuroMab; 75-136), rabbit anti-Plk2 (Thermo Scientific; PA5-14094), goat anti-E6TP1 (SPAR; Santa Cruz Biotechnology; N-20 sc-20846), rabbit anti-p65 (Santa Cruz Biotechnology; sc-372), and mouse anti HSC-70 (Santa Cruz Biotechnology; B-6 sc-7298). The following secondary antibodies were used: HRP-conjugated goat anti-mouse (Santa Cruz Biotechnology; sc-2314), goat anti-rabbit (Santa Cruz Biotechnology; sc-2054), and donkey anti-goat (Santa Cruz Biotechnology; sc-2020).

Reporter and kinase assays. NF-κB reporter assays were performed as described previously (Pomerantz et al., 2002; Meffert et al., 2003) using either HEK 293T cells or hippocampal cultures, as indicated. Inhibitor of NF-κB (IκB) kinase complex (IKK) activity assays were performed in HEK 293T cell lysates following infection (multiplicity of infection, ~10) with lentivirus encoding GFP-Plk2^{T236E} or GFP for 36 h. Twenty micrograms of lysate were reserved for input control, and 400 μg of lysate was immunoprecipitated (IP) with anti-IKK antibody (Imgenex; IMG-136; clone 14A231; mouse monoclonal) for 3 h at 4°C with rotation in the presence of phosphatase inhibitors. Prewashed protein A/G Sepharose beads were added to bind the antibody for 2 h with rotation at 4°C. Beads were then incubated with ^{32}P- γ-ATP^{32}P (6000 Ci/mmol; GE Healthcare) and purified substrate, GST-IκBα 1–62 wt, in 30 μl kinase reaction buffer for 30 min at 30°C. Kinase reaction buffer contained the following (in mM): 10 HEPES, pH 7.9, 5 $MgCl_2$, 1 $MnCl_2$, 12.5 β-glycerophosphate, 2 NaF, 50 Na_3VO_4, and 50 DTT. Reactions were terminated by addition of SDS-PAGE sample buffer and boiled for 3 min, and samples, including beads, were resolved by SDS-PAGE electrophoresis and transferred to PVDF membrane. The membrane was exposed in a phosphoimager cassette overnight and scanned with a Storm Phosphoimager (Molecular

Dynamics), followed by membrane rehydration and immunoblotting for normalization.

Confocal imaging and analysis. Confocal imaging and analysis were done essentially as described previously (Boersma et al., 2011). Spine density was measured in ImageJ from *Z*-stack projections containing the entire neuron or dendrite of interest. Spines were defined as protrusions 0.4–2.5 μm in length with or without a head. Secondary or tertiary dendritic branch segments were routinely selected for consistency. Automated analysis of dendritic protrusions was used to determine spine head volume by measuring a terminal-fitted sphere (Imaris 7.4; Bitplane). Endogenous synaptic GluA1 puncta were quantified by colocalization with puncta of low-level expressed PSD95-eBFP2 using the Imaris (Bitplane) colocalization function. Automated analysis of GluA1 and PSD-95 puncta was conducted using the spot detection function in Imaris. A quality filter and intensity median filter for the red channel (expressing untagged mCherry for dendrite visualization) were used during analysis to insure that quantification of puncta was restricted to those within the selected dendrite. A mask using a surface created in the red channel (from expressed mCherry fluorophore) was used to restrict puncta to those within selected representative dendrites only for visual presentation of synaptic GluA1 (see Fig. 6*G*). If required, for visual presentation only, levels of all imaged channels were adjusted equally (Adobe Photoshop), preserving relative fluorescence (see Fig. 6*G*).

Electrophysiology. Pyramidal neurons from DIV21 $RelA^{F/F}$ hippocampal cultures expressing GFP or Cre-IRES-dsRed for 48 h were mock or PTX treated (100 μM, 20–28 h) and subsequently chosen for whole-cell recordings by an experimenter blinded to the experimental conditions. Whole-cell recordings were performed using 7–9 MΩ glass electrodes filled with the following (in mM): 115 CsMeSO4, 0.4 EGTA, 5 tetraethylammonium-Cl, 2.8 NaCl, 20 HEPES, 3 Mg-ATP, 0.5 Na-GTP, and 10 Na-phosphocreatine, pH 7.2, 292 mOsm. Miniature EPSC (mEPSC) recordings were made without series resistance compensation in extracellular solution containing the following (in mM): 143 NaCl, 5 KCl, 10 HEPES, 10 glucose, 2 $CaCl_2$, 1 $MgCl_2$, 0.001 tetrodotoxin, 0.1 picrotoxin, and 0.2 DL-AP5, pH 7.4, 305 mOsm. Cells were voltage clamped at −70 mV during recording. Signals were digitized at 10 kHz and low-pass filtered at 2 kHz. Data were analyzed off-line (Mini Analysis; Synaptosoft) by an experimenter blinded to condition.

Chromatin immunoprecipitation. DIV21 dissociated neurons were transduced with lentivirus encoding GFP or the kinase-active GFP-$Plk2^{T236E}$ (multiplicity of infection, ~10) for 9.5 h. Expression from lentiviral constructs is undetectable by immunoblot before 6 h. Chromatin immunoprecipitation (ChIP) was performed with modifications (M. Kaileh, NIA, NIH, Bethesda, MD) of previously described protocols (Chowdhury and Sen, 2001; Wurster et al., 2011) using 3.3×10^6 neurons per IP. Following 2% formaldehyde cross-linking and glycine quench, cells were washed (HBSS; Invitrogen, catalog #14170), scraped, pelleted, and resuspended in cold HBSS (1 ml). Nuclei were prepared by lysing cells in buffer (4 ml) containing 10 mM Tris, pH 7.5, 320 mM sucrose, 5 mM $MgCl_2$, 1% Triton X-100, freshly added Roche protease inhibitors, and 2 PMSF. Nuclei were collected by centrifugation, resuspended in buffer containing 1% SDS, and used to generate sheared chromatin (average fragment size, 400 bp) for IP with anti-p65 antibody (Santa Cruz Biotechnology; sc-372) or rabbit IgG (Santa Cruz Biotechnology; sc-2027). The coprecipitated DNA was purified and analyzed by real-time PCR (SYBR Green; Bio-Rad, catalog #172-5121) using the following prevalidated primers: *SIPA1L1* (NM_001167983.1) promoter, forward, 5′ GGGAGACCGCCCGCAGCGTG 3′; reverse, 5′ CCGCGGGGGAGGGGACAGGTA 3′; control 5 kb 5′ of *SIPA1L1* transcriptional start site, forward, 5′ GTGGGATGTGATGACTGGCCTGGATGTG 3′; reverse: 5′ CACCTCATGGTGACCTTACCACG CTGGTG 3′.

ChIP data were analyzed as described previously (Chakraborty et al., 2007).

Statistical and bioinformatic analyses. For statistical analyses, two-tailed *t* tests (unpaired) were used with $\alpha = 0.05$ or one-way ANOVA followed by Bonferroni–Holm *post hoc* test where specified in the figure legends. Statistical significance of mEPSC cumulative distributions was determined using one-tail Kolmogorov–Smirnov (K–S) test. The Transcriptional Element Search System (TESS, University of Pennsylvania, Philadelphia, PA) was used for initial detection of putative NF-κB DNA-binding sites in *SIPA1L1* promoter.

Results

Neuronal Plks activate NF-κB through the canonical pathway

A member of the Plk family of serine/threonine kinases, Plk2, was identified in an expression-cloning screen for NF-κB activators using a placental cDNA library(Pomerantz et al., 2002). The importance of both NF-κB and Plks in neuronal plasticity prompted our further evaluation of this initial finding. Coexpression of an NF-κB luciferase reporter with increasing amounts of murine Plk2 resulted in significant and dose-dependent NF-κB activation (Fig. 1*A*) in heterologous cells. To control for transfection efficiency and extract recovery, luciferase activity was normalized to β-galactosidase activity expressed from a cotransfected constitutively active vector, Csk-LacZ. Significantly, a reporter in which mutation of the κB consensus binding site renders it nonresponsive to NF-κB (mtκB; see Materials and Methods) was not activated by Plk2 expression, demonstrating specificity of Plk2 expression for NF-κB-dependent transcription. We next addressed the role of the kinase activity of Plk2 in NF-κB induction. Expression of a mutant of Plk2 (T236E) with constitutive kinase activity produced relatively higher NF-κB activation than wild-type Plk2; this effect was most pronounced at lower Plk2 expression levels, consistent with a limiting role for Plk2 kinase activity in producing NF-κB activation (Fig. 1*B*). We conclude that Plk2 expression, and the kinase activity of Plk2, can specifically induce NF-κB activation.

To investigate whether Plks might regulate neuronal NF-κB, we tested the NF-κB reporter assay in primary murine hippocampal neurons with Plk2 and Plk3 expression, each of which undergo activity-responsive expression in neurons and possess highly conserved N-terminal serine/threonine kinase domains. Expression of Plk2 or Plk3 each produced significant and dose-dependent NF-κB activation (Fig. 1*C*) in DIV20 hippocampal cultures. We further evaluated the role of Plk kinase activity in producing NF-κB activation by comparing activation produced by wild-type Plks with kinase-dead mutants of Plk2 and Plk3; unlike wild-type Plks, the kinase-dead mutants did not activate NF-κB (Fig. 1*C*). Multiple serine-directed phosphorylation events are critical in the canonical NF-κB activation pathway, including activation of the IκB kinase complex and phosphorylation and degradation of the IκB. We used heterologous cells to test whether Plk kinase activity might regulate NF-κB through the canonical pathway. IP of the IKK complex from HEK 293T cells expressing the control flap-ubiquitin-promoter-GFP-WRE (FUGW) or GFP-tagged kinase-active Plk2 (Plk^{T236E}) followed by *in vitro* kinase assay showed that Plk2 induced IKK activation and phosphorylation of IκBα (Fig. 1*D*). Collectively, these data indicate that Plks activate neuronal NF-κB through a mechanism requiring Plk serine/threonine kinase activity and likely mediated through the canonical NF-κB activation pathway at or above the level of IKK.

Functional opposition of NF-κB and Plk2 determines spine density and surface excitatory receptor levels

Given that NF-κB generally enhances excitatory synaptic function and that Plks are known to attenuate synaptic excitation, we tested whether Plk induction of NF-κB might oppose and limit functional effects of Plks in neurons. While NF-κB is highly active in developing neurons during synaptogenesis, it is expressed at similar levels but primarily latent in mature neurons where it is

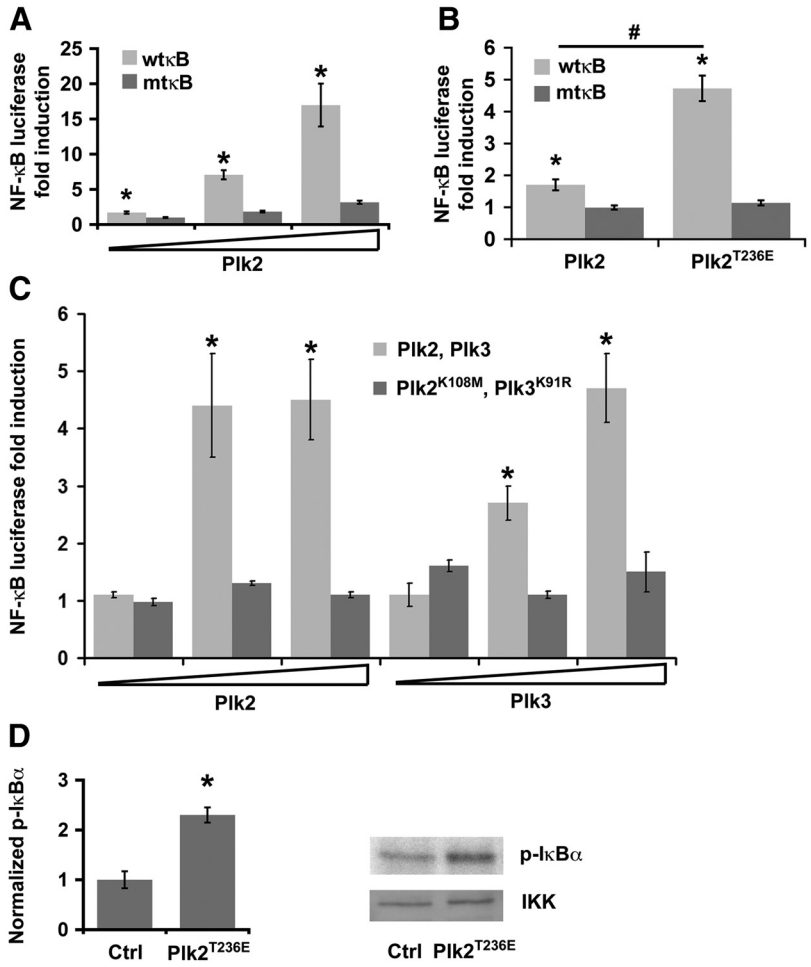

Figure 1. NF-κB is activated through the canonical pathway by Plks requiring intact kinase activity. ***A***, Plk2 specifically activates NF-κB in heterologous HEK 293T cells. Luciferase assay in cells transfected with reporters containing wild-type or mutant NF-κB binding sites and increasing amounts (10, 100, 300 ng) of wild-type Plk2 [$*p \leq 0.0003$ relative to Plk2 negative control (Ctrl); $n = 6$]. ***B***, Constitutively active Plk2 ^{T236E} activates NF-κB more robustly than wild-type Plk2 by luciferase assay in HEK 293T cells. Cells were transfected with wtκB or mtκB reporters and 10 ng of wild-type Plk2 or constitutively kinase active Plk2 ^{T236E} ($*p \leq 7.5 \times 10^{-4}$ relative to Ctrl; $^{\#}p = 1.55 \times 10^{-5}$; $n = 6$). ***C***, Neuronally expressed Plks activate NF-κB. NF-κB luciferase reporter assay in hippocampal neurons transfected with increasing amounts (0.5–1.0–2.0 μg) of wild-type or kinase-dead Plk mutants (Plk2 ^{K108M} and Plk3 ^{K91R}) is shown ($*p \leq 0.05$ relative to Ctrl; $n = 6$). ***D***, Plks activate NF-κB through the canonical pathway. IKK kinase assay in HEK 293T cells expressing GFP or GFP-Plk2 ^{T236E} from a lentivirus using GST-IκBα as a substrate. Phosphorylated IκBα is normalized to total immunoprecipitated IKK ($*p \leq 0.0001$; $n \geq 6$). All statistics are reported from at least three independent experiments. *n*, Number of independent biological replicates. Error bars indicate SEM.

available for stimulus-induced activation (Boersma et al., 2011). We took advantage of the low unstimulated NF-κB activity in mature neurons where synaptogenesis has plateaued (DIV21) to permit isolation of the interactive effects of Plks and NF-κB on excitatory synapses. Endogenous NF-κB levels were controlled using a characterized mouse strain carrying a loss of function allele for the *RelA* gene (encoding p65; *RelA*$^{F/F}$; Boersma et al., 2011). We demonstrated previously that loss of p65 in hippocampal neurons, where it is a predominant subunit, is sufficient to effectively inhibit NF-κB activation (Meffert et al., 2003; Boersma et al., 2011). Dendritic spines, the postsynaptic sites of excitatory synapses, are downregulated in response to Plk expression (Pak and Sheng, 2003). Interactions between Plk2 and NF-κB in the control of spine density were evaluated by expression of Plk2 in DIV21 hippocampal pyramidal neurons from *RelA*$^{F/F}$ mice expressing 4- OHT-inducible CreER^{T2} from a lentiviral vector (see Materials and Methods); similar results were obtained with expression of wild-type Plk2 or kinase-active Plk2 ^{T236E}, and these data were pooled (Fig. 2*A*). As anticipated, loss of p65 (OHT) alone had no effect on spine density in these mature neurons, while expression of Plk2 resulted in a modest but significant reduction in spine density (reduced by 1.97 spines/10 μm from control; $p = 1.2 \times 10^{-5}$, ANOVA; Fig. 2*A*). Importantly, Plk2 expression in the absence of p65 (OHT/Plk2; Fig. 2*A*) resulted in a highly significant ($^{**}p = 1.83 \times 10^{-6}$, ANOVA) additional loss of dendritic spines (reduced by 3.95 spines/10 μm from control; Fig. 2*A*). Overall, dendritic spines were reduced to 77% of control by Plk2 expression, and to 53.9% of control by Plk2 expression in the absence of p65. These results are consistent with NF-κB activation by Plk2 expression normally serving to balance and limit the extent of dendritic spine loss, an effect that is revealed by inducing deficiency of endogenous NF-κB.

To further explore functional opposition by NF-κB of Plk-mediated reduction in neuronal excitation, we used biotinylation assays to evaluate potential interactive effects on the surface and total expression of excitatory glutamate receptors in DIV21 hippocampal neurons. Loss of NF-κB alone (OHT) produced no reduction in either surface or total levels of the GluA1 AMPA receptor subunit. Plk2 expression had no significant effect on total GluA1, but produced a modest but significant reduction in surface GluA1 (Fig. 2*B*), consistent with previous reports (Evers et al., 2010). Plk2 expression in the absence of p65 (OHT/Plk2), however, produced robust loss of both total and surface neuronal GluA1 levels, resulting in a further 28.6% reduction of surface GluA1 and a reduction of total GluA1 by 34.7% compared to Plk2 expression in p65-wild-type neurons. Neither Plk2 expression nor loss of NF-κB significantly altered the ratio of surface to total GluA1 (Fig. 2*C*), potentially reflecting the fact that GluA1 expression is NF-κB dependent (Yu et al., 2002). In addition, biotinylation assays showed that neither Plk2 nor loss of NF-κB affected surface or total expression of inhibitory $GABA_A$ receptors (Fig. 2*D*). We conclude that Plk2 activation of NF-κB constitutes a counterforce that limits reductions in excitatory synapse function caused by Plk2, and could potentially dampen overshooting during homeostasis to allow fine-tuning of neuronal excitation.

Functional opposition of NF-κB and Plk regulates synaptic strength following periods of high activity

Expression of neuronal Plk2 is low under basal conditions and rapidly induced by periods of intense synaptic activity as part of the homeostatic response. To investigate whether opposing actions of Plk2 and NF-κB might determine the activity end points of homeostatic responses, we exposed neurons to enhanced excitatory activity using PTX, an antagonist of $GABA_A$ chloride channels, at a dose and duration previously used to study homeo-

static responses to elevated activity (Lee et al., 2011; Sun and Turrigiano, 2011). Immunoblot of lysates from DIV21 *RelA*$^{F/F}$ hippocampal cultures transduced with lentivirus expressing CreER^{T2} and treated with PTX (100 μM PTX, 24 h) showed an equivalent elevation of Plk2 protein in both p65-wild-type (PTX) and p65-deficient conditions (OHT/PTX; Fig. 3*A*), indicating that p65-deficient cultures undergo similar Plk2 induction and are suitable for studies of this homeostatic response. Chronic elevated neuronal activity (PTX) results in Plk2-dependent NF-κB activation, as assessed by reporter assay, which is blocked by expression of kinase-dead Plk2 (Plk2^{K108M}; Fig. 3*B*) that functions as a dominant negative (Pak and Sheng, 2003).

A reduction in dendritic spine size and density comprises part of the neuronal adaptive response to periods of high excitatory activity, such as is induced by PTX. We investigated potential effects of endogenous NF-κB on the homeostatic response of spines to elevated activity using live confocal imaging of mature (DIV21, at low basal NF-κB activity) *RelA*$^{F/F}$ neurons transfected with mCherry fluorophore for morphological visualization, with or without Cre cotransfection. As anticipated, exposure to heightened activity (PTX) resulted in a significant decline in both dendritic spine density (Fig. 3*C*) and spine head volume (*D*) relative to control conditions. While p65-deficiency alone (Cre) produced no significant change in either spine density or head volume compared to control (Fig. 3*C–E*), neurons lacking p65 responded to heightened activity with a substantially larger decrease in both dendritic spine density and volume than the response in control, p65-wild-type, neurons. The absence of p65 allowed chronic activity to decrease the spine density from 5.33 ± 1.26/10 μm (PTX alone) to 3.68 ± 1.17/10 μm (Cre/PTX) and more than doubled the decrease in spine head volume, from 0.142 ± 0.038 μm^3 (PTX alone) to 0.062 ± 0.029 μm^3 (Cre/PTX). These results indicate that NF-κB activation evoked by chronic synaptic excitation and consequent Plk induction provide an opposing balance to limit homeostatic reduction of dendritic spines.

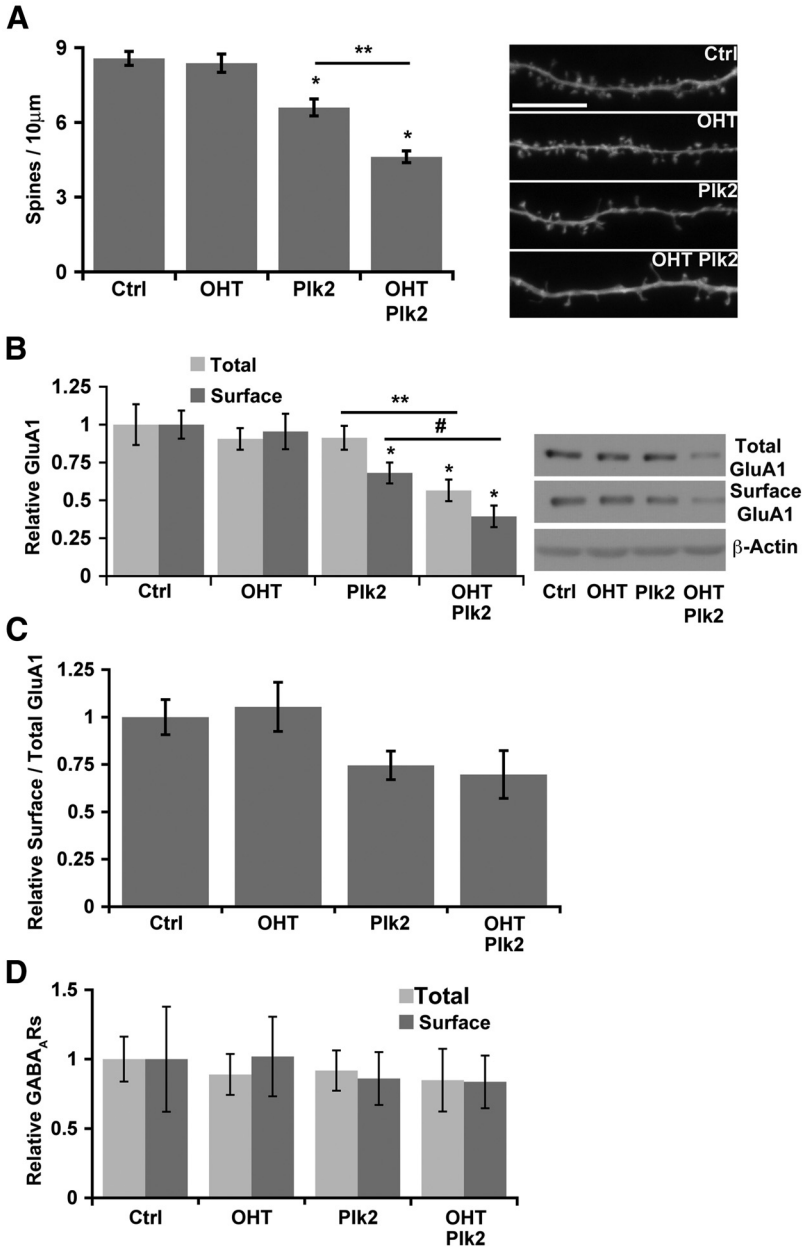

Figure 2. NF-κB and Plk interaction determines neuronal spine density and excitatory neurotransmitter receptor composition. ***A***, Neuronal NF-κB opposes and limits Plk2-induced spine loss. Average spine densities (left) quantitated from confocal projections of dendrites (representative segments; right) from DIV21 *RelA*$^{F/F}$ murine cultured hippocampal neurons transduced with CreER^{T2} by lentivirus infection and treated with vehicle or OHT to induce p65-deficiency. Plk2 (either wild-type or kinase-active with data pooled) was expressed for 24 h (*$p \leq 1.2 \times 10^{-5}$ relative to Ctrl; **$p = 1.83 \times 10^{-6}$, ANOVA; $n \geq 44$ dendritic segments from ≥10 independent experiments). Scale bar, 10 μm. ***B***, NF-κB limits Plk2-induced loss of surface GluA1 AMPA receptor subunits in hippocampal neurons. Averages of normalized total and surface GluA1 quantitated by densitometry (left) from immunoblots (representative blots; right) after surface biotinylation from DIV21 neurons in the presence (Ctrl) or absence of p65 (OHT) are shown, and wild-type Plk2 was transduced by lentiviral infection. β-Actin was used as the loading control (*$p \leq 0.012$ relative to Ctrl; **$p = 0.004$; #$p = 0.009$, ANOVA; $n \geq 7$ independent experiments). ***C***, Surface to total GluA1 ratio does not significantly change with Plk2 overexpression in wild-type or p65 deficient neurons (data from same experiments as in *B*). ***D***, NF-κB and Plk2 do not regulate inhibitory GABA$_A$ receptors in neurons (biotinylation assay as is Fig. 1*B*). Densitometric quantification of average surface and total GABA$_A$Rs. All error bars indicate SEM.

The induction of Plk2 expression by prolonged neuronal excitation is required for homeostatic reduction in synaptic currents(Seeburg and Sheng, 2008; Seeburg et al., 2008). To test whether NF-κB might also oppose the role of Plk2 in homeostatic reduction of excitatory responses, we performed whole-cell voltage-clamp recordings on hippocampal pyramidal neurons (DIV21) expressing GFP (control) or Cre recombinase plus dsRed (Cre; Cre-IRES-dsRed) and either untreated or exposed to PTX (100 μM, 20–28 h). mEPSC recordings were made in the presence of TTX, PTX, and DL-APV (NMDA receptor antagonist); representative traces for each condition are shown in Figure 4*A*. The average amplitude of mEPSCs recorded from neurons treated with PTX or Cre/PTX were both sig-

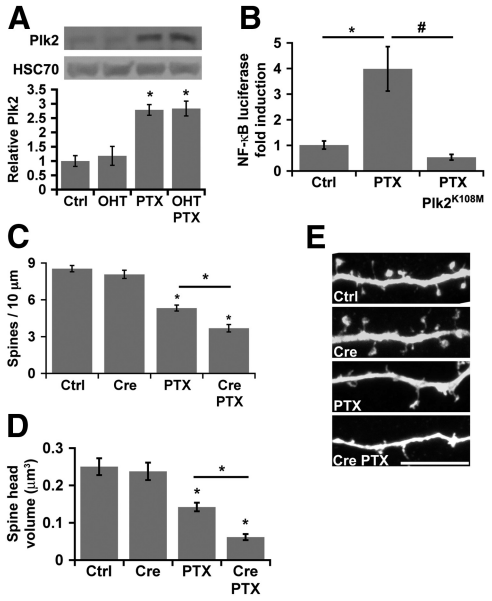

Figure 3. Hyperactivity induces Plk2 which is required for hyperactivity induction of NF-κB. ***A***, Representative immunoblot (inset) and quantification of Plk2 levels in lysates from chronic PTX (PTX, 100 μM, 24 h) or mock-treated DIV21 hippocampal cultures in the presence (Ctrl or PTX) or absence of p65 (OHT or OHT/PTX). HSC70 was used as the loading control ($*p \leq 4.54 \times 10^{-4}$, ANOVA; $n = 5$ independent experiments). ***B***, NF-κB luciferase reporter in DIV19 hippocampal neurons. NF-κB transcriptional activity is significantly increased by 12 h PTX treatment (50–100 μM; $*p = 0.003$), but this is prevented by expression of the kinase-dead Plk2^{K108M} ($^{\#}p = 0.01$; $n = 3$ independent experiments). ***C***, NF-κB limits decreases in spine density by chronic PTX. Hippocampal neurons (DIV21, *RelA*$^{F/F}$ mice) in the presence or absence of p65 (Cre expression 48 h) were vehicle or PTX treated (100 μM for 24 h; $*p \leq 1.62 \times 10^{-4}$, ANOVA; $n \geq 15$ dendritic segments from 4 independent experiments). ***D***, NF-κB limits decreases in spine volumes by chronic PTX. Spine head volumes were measured using Imaris software from the same dendritic segments as in ***A*** ($*p \leq 5.42 \times 10^{-4}$, ANOVA). ***E***, Confocal projections of representative dendrite segments for data in ***C*** and ***D***. Scale bar, 10 μm. All error bars indicate SEM.

nificantly reduced compared to the amplitude of mEPSCs from control neurons (PTX, $n = 10$, $p = 0.008$; Cre/PTX, $n = 11$, $p = 5.57 \times 10^{-5}$, ANOVA; Fig. 4*B*). Importantly, the average amplitude of mEPSCs recorded from PTX-treated neurons lacking p65 (Cre/PTX) was significantly further reduced compared to PTX-treated neurons harboring wild-type levels of p65 ($p = 0.023$, ANOVA; Fig. 4*B*). In the absence of PTX, mEPSC average amplitudes did not significantly differ between control neurons and neurons lacking p65 (Cre, $n = 10$, $p = 0.675$, ANOVA; Fig. 4*B*). As expected, elevated activity also induced a left shift in the cumulative distribution of mEPSC amplitudes compared to control values (Fig. 4*C*; Ctrl compared to PTX, $p = 0.014$ by K–S test). Notably, there was a further significant left shift in the cumulative distribution of mEPSC amplitudes between PTX-treated wild-type (PTX) and p65-deficient neurons (Cre/PTX) (Fig. 4*C*, right; $p = 0.008$ by K–S test), indicating that spontaneous synaptic responses are consistently further reduced at all amplitudes in response to elevated activity in the absence of p65. Collectively, these results indicate that endogenous NF-κB exerts a positive regulation of excitatory AMPA receptor-mediated currents that counteracts homeostatic downregulation by chronic excitation, and are consistent with a role for NF-κB in balancing neuronal responses to determine the equilibrium end points of excitation in homeostatic plasticity. The observed enhancement of synaptic function is consistent with our data that active NF-κB positively regulates spine head volume during the homeostatic response to chronic excitation (Fig. 3*D*). We conclude that NF-κB is activated by Plk induced during intense excitation, and that this NF-κB activation serves to counter and restrain homeostatic downregulation of excitatory synapses at both structural and functional levels.

Given that NF-κB also positively regulated spine density during the homeostatic response to chronic activity (Fig. 3*C*), a reduced frequency of mEPSCs in PTX-treated neurons lacking p65 might also be anticipated. Recordings from PTX-treated neurons lacking p65 (Cre/PTX) demonstrated a trend toward reduced average mEPSC frequency compared to PTX-treated neurons not expressing Cre (PTX), but these results did not reach significance (Fig. 4*D*). One potential explanation for this finding lies in the relatively high cell-to-cell variability of mEPSC frequency across cultures. Indeed, the coefficient of variation for mEPSC frequency within control neurons ($C_V = 0.766$) far exceeds that for mEPSC amplitude ($C_V = 0.119$), indicating that experimental sensitivity for changes in amplitude is greater. mEPSC frequency was also analyzed by cumulative distribution plot of interevent interval (IEI; Fig. 4*E*). The cumulative IEI is significantly right-shifted from control by PTX exposure in the absence of p65 (Cre/PTX, $p = 0.018$), and the difference in IEI between neurons exposed to elevated activity (PTX) in the presence or absence of p65 is also significant ($p = 0.035$), as analyzed by one-tailed K–S test performed with the assumption that mEPSC IEIs are greater in Cre/PTX than PTX alone.

Opposing actions of Plk2 and NF-κB-mediated transcription converge to determine SPAR protein levels

We next sought to identify a downstream mechanism by which antagonistic effects of Plks and NF-κB might shape the equilibrium end point of homeostatic responses to elevated excitation. Plk2 expressed in response to elevated synaptic activity is preferentially enriched at dendritic spines where it triggers the phosphorylation and subsequent ubiquitination and degradation of SPAR, a synapse-stabilizing protein (Pak et al., 2001; Pak and Sheng, 2003; Ang et al., 2008). SPAR elimination is required for reduction in the number and size of mature dendritic spines and excitatory synapses by Plk2 (Pak and Sheng, 2003; Lee et al., 2011). To investigate whether regulation by Plk2 and NF-κB might converge on SPAR, we first examined SPAR protein levels by immunoblot from lysates of mature DIV21 hippocampal neurons expressing Plk2 in the presence or absence of p65. As expected since NF-κB is relatively inactive in mature neurons under basal conditions, loss of p65 alone (OHT) did not alter SPAR protein levels from control neurons (Ctrl; Fig. 5*A*). Expression of Plk2 (which activates NF-κB; Fig. 1) resulted in a significant decrease of SPAR protein relative to control neurons that was greatly amplified in the absence of p65 (OHT/Plk2; Fig. 5*A*). SPAR protein levels were decreased to 66.2 ± 0.07% of control by Plk2 expression in p65-wild-type neurons, and to 26.7 ± 0.08% of control by Plk2 expression in p65-deficient neurons.

To investigate whether NF-κB might regulate SPAR in a transcriptional or posttranscriptional manner, we first took advantage of the fact that NF-κB is highly transcriptionally active during developmental periods of synaptogenesis both *in vivo* and *in vitro* (DIV7–DIV18), compared to basal activity levels in mature neurons (Fig. 5*B*, compare DIV16, DIV21). Loss of p65 from hippocampal neuronal cultures when NF-κB is highly transcriptionally active (DIV16) resulted in a significant decrease in SPAR protein levels that could be rescued by expression of exogenous p65 (Fig. 5*C*). NF-κB is also highly active *in vivo* during periods of active synaptogenesis. We introduced GFP-Cre or GFP to developing hippocampal neurons of *RelA*$^{F/F}$ P0 mouse pups by lateral

ventricle AAV injection and assessed the effects on *in vivo* SPAR expression 13 d later (Fig. 5*D*). Loss of p65 significantly decreased *in vivo* SPAR expression as assessed by immunoblot of hippocampal lysates (Fig. 5*D*). Imaging for GFP in cryosections and immunoblotting demonstrated successful targeting of >50% of hippocampal neurons by AAV injection (Fig. 5*E*,*F*) with effective recombination and loss of p65 (Fig. 5*D*). These results indicate that active NF-κB critically controls SPAR levels both *in vitro* and *in vivo*.

These findings suggested that NF-κB-dependent transcriptional activity might be responsible for SPAR upregulation by NF-κB. Analysis of the promoter region of the murine *SIPA1L1* gene encoding SPAR protein (transcript variant 2, NCBI reference sequence NM_001167983.1) revealed multiple putative binding sites for NF-κB, including three sites within 500 bp upstream of the predicted transcriptional start site and one perfectly matched consensus site at +524 from the predicted transcriptional start site. Examination of the promoter region for rat and human genes encoding SPAR protein reveals limited direct sequence conservation with mouse; however, each contains consensus sites for NF-κB binding upstream of the transcriptional start sites. The effect of NF-κB on the *SIPA1L1* promoter was tested by cloning ~1.2 kb of the promoter region (−508 to +688; containing the predicted NF-κB binding sites) upstream of a promoterless luciferase reporter. Cotransfection of this *SIPA1L1* reporter with a titration of p65-expression vector in HEK 293T cells resulted in significant and dose-dependent activation (Fig. 6*A*). All luciferase activities were normalized to a cotransfected constitutive β-galactosidase reporter (see Materials and Methods). These results further indicated transcriptional regulation of SPAR by NF-κB. We analyzed binding of NF-κB to the *SIPA1L1* promoter by ChIP in dissociated hippocampal neurons, expressing either GFP or GFP-Plk2^{T236E} (see Materials and Methods). We detected binding of NF-κB (p65 subunit) to sequences 1 kb 5′ of the transcriptional start site for SPAR in a region containing three putative NF-κB sites (TESS). Plk2 induced a 2.4-fold increased association of NF-κB with the *SIPA1L1* promoter, compared with control, GFP-expressing neurons (Fig. 6*B*, left). In contrast, we did not detect binding of NF-κB (p65 subunit) to sequences 5 kb 5′ of the transcriptional start site for SPAR, which lacks putative NF-κB DNA binding sites; Plk2 expression also did not influence binding at this genomic site (Fig. 6*B*, right). Collectively, these data are consistent with direct targeting of the *SIPA1L1* promoter by NF-κB.

Targeted protein degradation is a primary mechanism controlling SPAR levels. To assess the possibility that NF-κB might also influence the stability of SPAR protein, we evaluated the effects of loss of NF-κB on a SPAR fusion protein expressed from a construct containing only the coding sequence of SPAR fused to luciferase (see Materials and Methods) to allow highly sensitive and quantitative detection of SPAR in the absence of influence from the endogenous *SIPA1L1* promoter. Titrated expression of this construct in p65-deficient or wild-type hippocampal neurons (at DIV16, when loss of p65 regulates endogenous SPAR under basal conditions) revealed no effect on the levels of SPAR protein (Fig. 6*C*). Collectively, these experiments define a mechanism of SPAR coregulation by Plk2 and NF-κB, with Plk2 regulating the stability of the SPAR protein and NF-κB acting at the level of SPAR transcription.

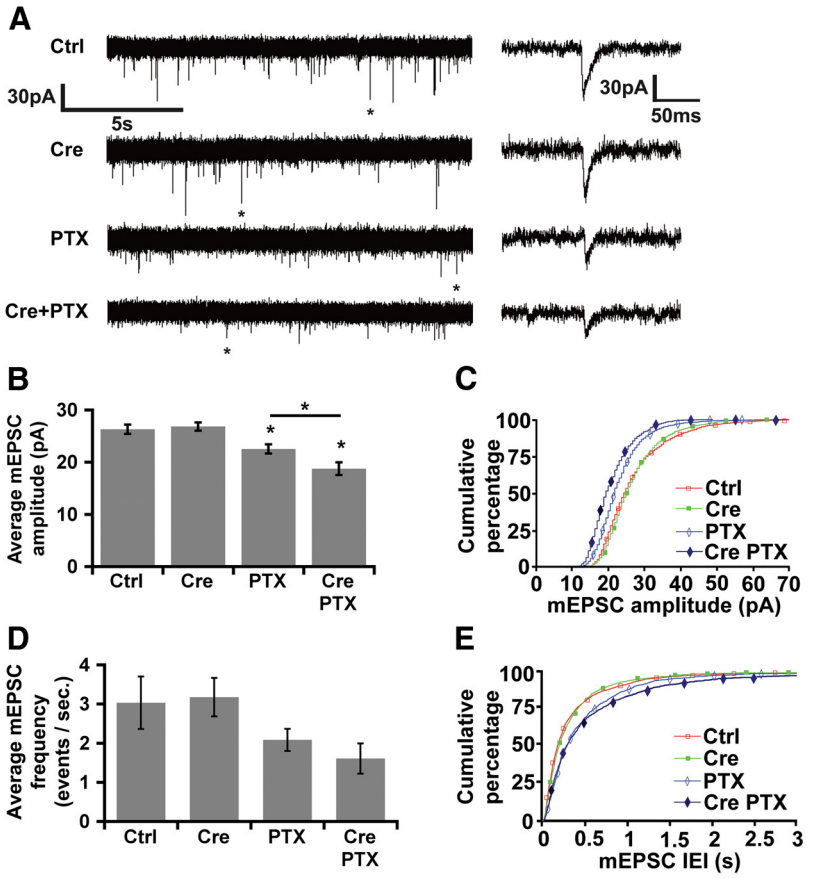

Figure 4. NF-κB opposes the homeostatic downregulation of synaptic strength by elevated activity. ***A***, Representative traces of mEPSCs recorded from p65-wild-type or p65-deficient (Cre) DIV21 *RelA*$^{F/F}$ hippocampal cultures after treatment with vehicle or PTX (100 μM for 20–28 h). Right, Enlarged single events (marked by asterisks) from each condition. ***B***, NF-κB limits the homeostatic decrease in AMPAR-dependent mEPSC amplitudes in response to elevated activity in hippocampal neurons. Average AMPAR-dependent mEPSC amplitudes under the indicated conditions (*$p \leq 0.023$, ANOVA). ***C***, Cumulative percentage plot of mEPSC amplitudes from all recorded neurons ($n_{Ctrl} = 12$, $n_{Cre} = 10$, $n_{PTX} = 10$, $n_{Cre+PTX} = 11$, where *n* represents individual neurons recorded from 10 independent experiments). K–S statistical analysis shows a significant left shift in the cumulative distribution of mEPSC amplitudes from Ctrl after chronic PTX both in the presence (PTX; $p = 0.014$) and absence of p65 (Cre/PTX; $p = 9.67 \times 10^{-4}$). There is also a statistically significant left shift in the cumulative distribution of mEPSC amplitudes in neurons treated with PTX in the absence of p65 (Cre/PTX) compared to neurons with p65 (PTX; $p = 8.65 \times 10^{-3}$). ***D***, Average AMPAR-dependent mEPSC frequency under the indicated conditions. ***E***, Cumulative percentage plot of mEPSC IEIs from all recorded neurons. K–S test shows statistically significant right shifts from Ctrl in the cumulative distribution of mEPSC IEIs after chronic PTX in the absence of p65 (Cre/PTX; $p = 0.018$), and between chronic PTX in the presence (PTX) and absence of p65 (Cre/PTX; $p = 0.035$), but there is no statistical difference from Ctrl in the presence of PTX (PTX; K–S test). All error bars indicate SEM.

SPAR rescues the effects of loss of NF-κB

To further evaluate the importance of SPAR as a target for NF-κB in homeostatic plasticity, we attempted to rescue the effects of loss of p65 by exogenous expression of murine SPAR in neurons exposed to chronic activity (PTX, 100 μM 24 h). SPAR expression fully rescued the additional loss of dendritic spine head volume

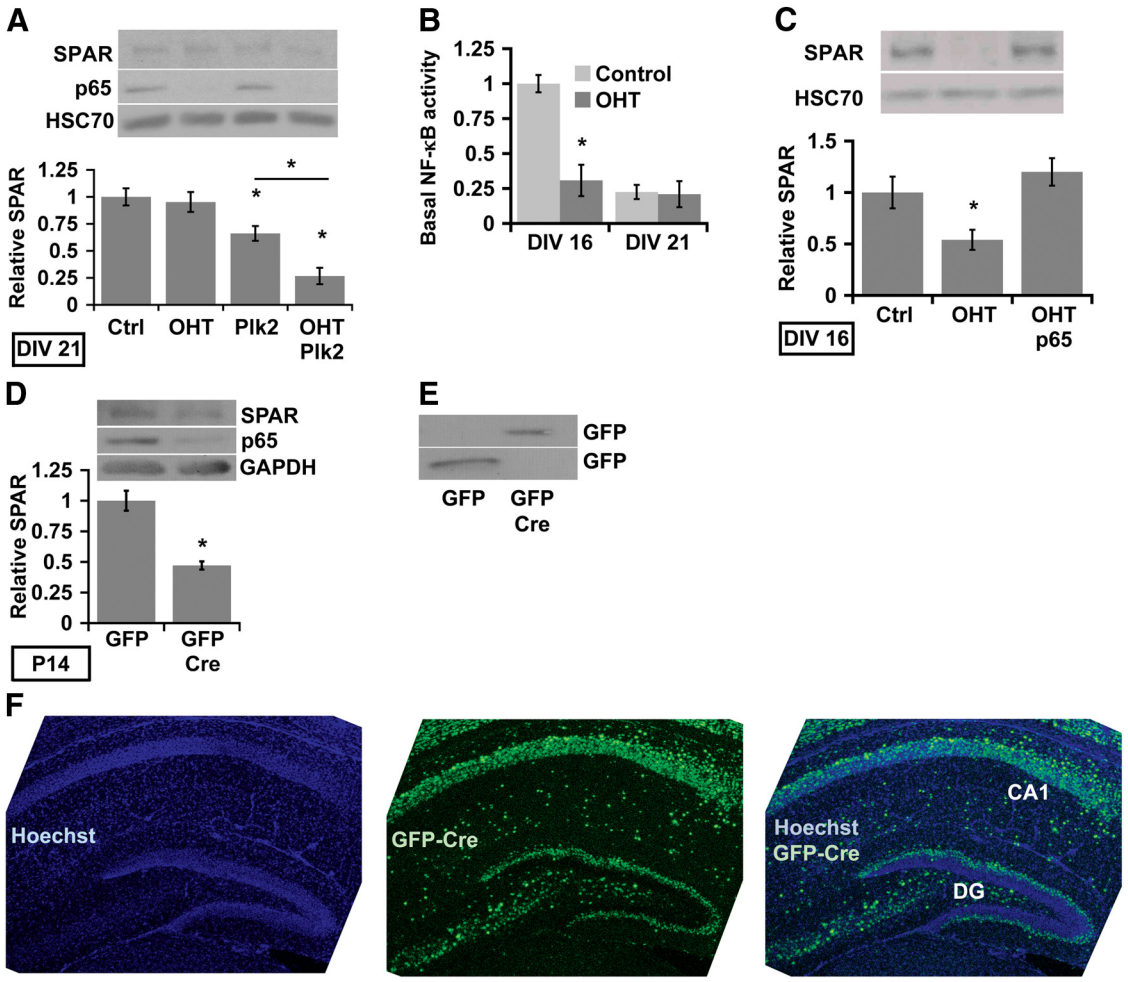

Figure 5. NF-κB positively regulates SPAR protein *in vitro* and *in vivo*. ***A***, NF-κB limits Plk2-induced SPAR protein loss in neurons. Representative immunoblot (inset) and quantification of SPAR levels in lysates from mock or Plk2 infected (lentivirus, 2 d) DIV21 hippocampal cultures in the presence (Ctrl) or absence of p65 (OHT). HSC70 was used as the loading control (*$p \leq 2.87 \times 10^{-3}$, ANOVA; $n = 5$ independent experiments). ***B***, ***C***, Levels of neuronal SPAR positively correlate with NF-κB activity. ***B***, NF-κB reporter assay shows that NF-κB activity is higher in developing (DIV16) compared to mature (DIV21) hippocampal cultures. ***C***, Representative immunoblot and quantitated levels of SPAR protein in DIV16 $RelA^{F/F}$ hippocampal cultures in the presence (Ctrl) or absence (OHT) of p65, or following rescue of p65-deficiency by expression of exogenous p65 (OHT/p65; using lentiviral expression of Myr-GFP-F2A-p65). Average data are plotted normalized to Ctrl. HSC70 was used for the loading control (*$p \leq 0.04$; $n \geq 3$ independent experiments). ***D***, Representative immunoblot (inset) and normalized quantification of SPAR protein levels in $RelA^{F/F}$ P14 mice transduced with control GFP or GFP-Cre by AAV injections at P0. SPAR levels are significantly reduced ($p = 2.07 \times 10^{-4}$; $n_{GFP} = 3$, $n_{GFP\text{-}Cre} = 6$ mice) by *in vivo* NF-κB deficiency. ***E***, Immunoblot showing expression of GFP and GFP-Cre from $RelA^{F/F}$ hippocampi transduced with AAV injected at P0 and harvested at P14. ***F***, Confocal *Z*-stack projections of a P12 mouse hippocampus showing viral expression of GFP-Cre following P0 lateral ventricle AAV injections. Hippocampi were cryosectioned after harvest at P12 with Hoechst dye used to counterstain nuclei. We observe >50% infection efficacy of neurons in the hippocampal pyramidal layer (CA1 shown in image) and in the dentate gyrus (DG). All error bars indicate SEM.

observed in neurons exposed to chronic activity in the absence of p65 (Cre/PTX/SPAR); p65-deficient neurons expressing SPAR no longer had a significant difference in spine volume response to chronic activity when compared to p65-wild-type neurons (PTX; Fig. 6*D*); and expression of SPAR in untreated p65-deficient neurons (Cre/SPAR) did not significantly alter spine head volume compared to control untreated neurons (100%; Fig. 6*D*). The reduction of synapse-localized AMPA glutamate receptors is a critical component of the neuronal homeostatic response to elevated activity. As anticipated, levels of synaptic GluA1, quantified by colocalization with dendritic spine PSD-95 (see Materials and Methods) in DIV21 pyramidal neurons, were reduced by 24 h treatment with PTX (Fig. 6*E*). Importantly, elevated neuronal activity resulted in a significantly greater reduction of synaptic GluA1 in p65-deficient neurons compared to p65-wild-type neurons ($p = 0.027$; $n = 11$ PTX; $n = 11$ Cre/PTX; Fig. 6*E*,*F*). We next asked whether SPAR expression could rescue synaptic GluA1 content to appropriate levels in p65-deficient neurons responding to chronic activity. Expression of SPAR in p65-deficient neurons exposed to PTX (Cre/PTX/SPAR; Fig. 6*E*,*F*) restored synaptic GluA1 to levels that were not significantly different from synaptic GluA1 in p65-wild-type neurons responding to chronic activity (PTX; $p = 0.156$; Fig. 6*E*,*F*); SPAR expression in p65-deficient neurons not exposed to elevated activity did not significantly alter synaptic GluA1 levels (Cre/SPAR; Fig. 6*E*,*F*). These experiments indicate that expression of SPAR is sufficient to counteract the effects of loss of NF-κB on both spine volumes and synaptic AMPARs during homeostatic plasticity. Collectively, our data support SPAR as an NF-κB target gene that plays a central role in NF-κB function as an antagonizing force acting to curtail synapse loss and maintain synaptic function during homeostatic plasticity to chronic heightened activity. The opposing influences of Plks and NF-κB, both induced by heightened neuronal activity, act to determine

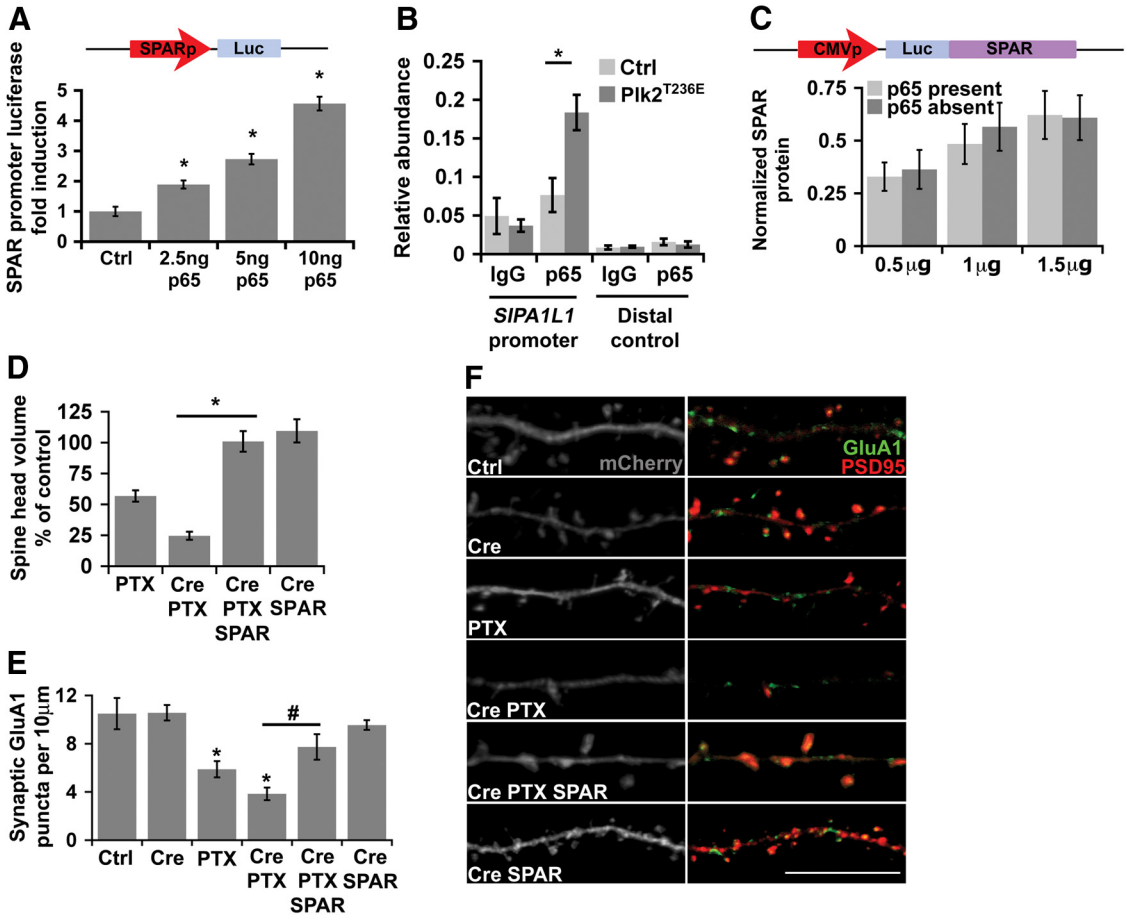

Figure 6. SPAR is transcriptionally upregulated by NF-κB and rescues the decrease in synaptic strength due to loss of p65 in neurons exposed to hyperactivity. ***A***, NF-κB induces a reporter driven by the SPAR promoter assayed in HEK 293T cells. Diagram (top inset) of SPAR promoter luciferase reporter, with ~1.2 kb flanking the mouse SPAR transcriptional start site, containing four putative κB DNA binding sites. Plot of reporter assay in cells transduced with 0 to 10 ng of p65 subunit of NF-κB (*$p \leq 0.01$; $n = 3$ independent experiments). ***B***, NF-κB induction by Plk2 leads to an increased association of p65 with *SIPA1L1* promoter in hippocampal neurons. ChIP assays were performed with either anti-p65 antibody or isotype-matched IgG, in DIV21 hippocampal dissociated cultures expressing either GFP (Ctrl) or GFP-tagged constitutively active Plk2^{T236E}; using either primers within the *SIPA1L1* promoter (left) or upstream control primers (right; *$p = 0.008$; $n = 5$ independent experiments). The relative abundance of specific amplicons in the IP compared to the input DNA is shown on the *y*-axis. ***C***, NF-κB does not regulate SPAR protein levels from a construct lacking the endogenous SPAR promoter in neurons. Inset, Diagram of construct containing the SPAR coding sequence fused directly to luciferase to allow sensitive quantification, and driven by a constitutive CMV promoter. SPAR protein level is quantified by luciferase activity from *RelA*$^{F/F}$ DIV16 dissociated hippocampal cultures transfected with a dose titration of the fusion construct in the presence or absence of p65. ***D***, Expression of exogenous SPAR rescues the overshoot of spine head volume loss in p65-deficient (Cre) neurons exposed to elevated activity. Average spine head volumes after chronic PTX are plotted as a percentage of control neurons (100%) not exposed to PTX to illustrate that low levels of SPAR expression rescue the exaggerated loss of spine volume in p65-deficient neurons exposed to elevated activity (*$p = 1.87 \times 10^{-8}$, ANOVA; Cre/PTX/SPAR; $n \geq 10$ dendritic segments from 4 independent experiments), but do not alter average spine volumes without heightened activity (Cre/SPAR). ***E***, Exogenous SPAR expression opposes excessive loss of surface synaptic GluA1 in response to elevated activity (PTX) in p65-deficient (Cre) neurons. Plot of average surface synaptic GluA1 density for the indicated conditions. Synaptic GluA1 was quantified (Imaris, Bitplane) from confocal images as surface GluA1 puncta colocalized with transfected PSD95 puncta in DIV21 *RelA*$^{F/F}$ hippocampal pyramidal neurons (*$p \leq 3.39 \times 10^{-3}$, #$p = 2.16 \times 10^{-3}$, ANOVA; $n \geq 10$ dendritic segments from 4 independent experiments). ***F***, Representative confocal projections of dendrites from pyramidal neurons for the indicated conditions, as quantified in ***D*** and ***E***. Right panels are masked (Imaris) for ubiquitously expressed mCherry fluorophore (left) to allow confirmation by visual inspection that illustrated puncta are within the presented dendritic segments. Scale bar, 10 μm. All error bars indicate SEM.

SPAR protein levels and the equilibrium end point of the homeostatic response.

NF-κB determines SPAR protein levels during the homeostatic response to elevated synaptic activity

Neuronal induction of Plks by chronic elevated activity is known to cause homeostatic reduction in both SPAR levels and synaptic responses; our data show that the Plk response also induces a balancing force through NF-κB activation. To determine whether NF-κB regulation of SPAR might be physiologically relevant in this homeostatic response, we first evaluated a role for NF-κB in determining SPAR protein levels following prolonged activity. *RelA*$^{F/F}$ murine hippocampal cultures (DIV21) in the presence or absence of p65 (OHT) were treated with PTX (100 μM, 24 h), and lysates were immunoblotted for SPAR. A representative blot (Fig. 7*A*) and quantitation (*B*) show that chronic activity reduces levels of SPAR protein, as expected, and that the SPAR reduction is significantly greater following PTX exposure when neurons are deficient for NF-κB ($p = 3.39 \times 10^{-3}$, ANOVA). Evaluation of the kinetics of this dual response through immunoblots and reporter assays reveals that heightened neuronal activity (PTX; 100 μM) induces an initial elevation of Plk protein and a corresponding overshoot in loss of SPAR protein (3 h; Fig. 7*C*,*E*,*F*). This period is followed by a slower induction of NF-κB-dependent transcription, first significant at 7 h and further elevated by 12–24 h (Fig. 7*D*), and a recovery of SPAR protein levels by 24 h to an intermediate level that is both significantly lower than baseline and also significantly higher (~48% recovery) than early time points following heightened activity (Fig. 7*E*,*F*). This time course is consistent

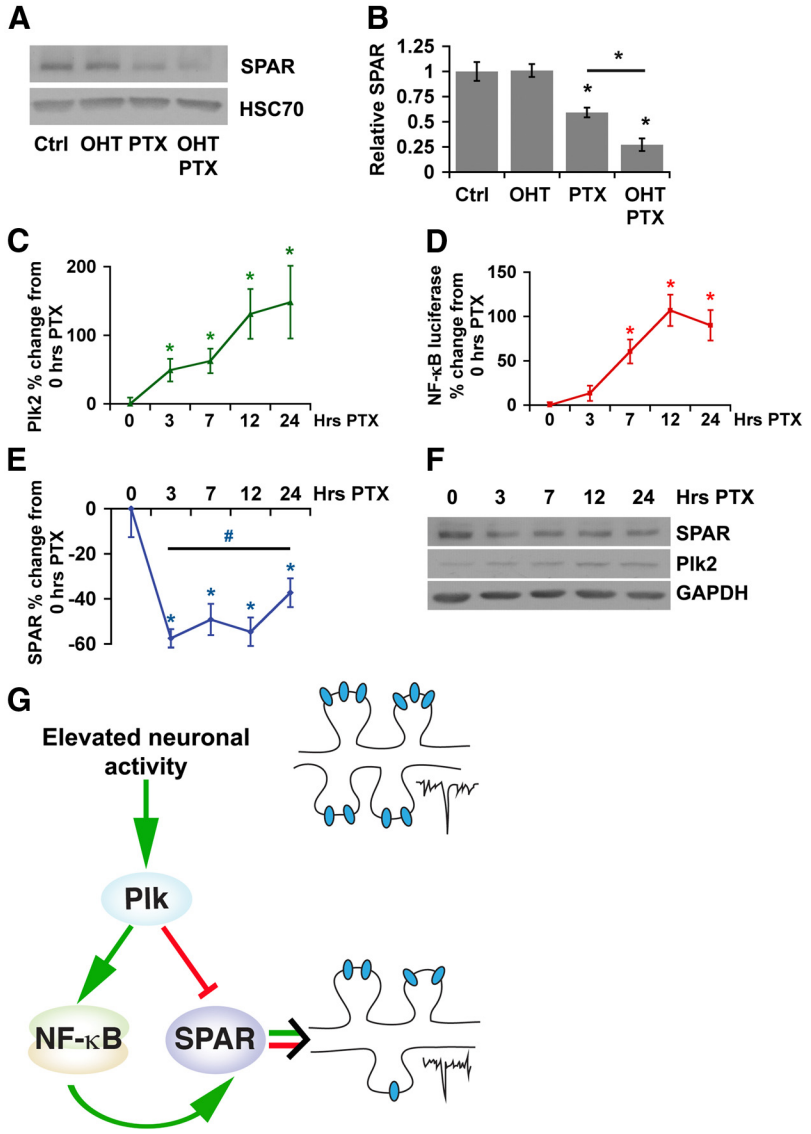

Figure 7. NF-κB, Plk2, and SPAR kinetics during PTX-induced hyperactivity. ***A***, ***B***, NF-κB limits the homeostatic SPAR loss in response to elevated activity in neurons. Representative immunoblot (***A***) and quantification (***B***) of SPAR levels in lysates from chronic PTX or mock-treated DIV21 hippocampal cultures in the presence (Ctrl or PTX) or absence of p65 (OHT or OHT/PTX). HSC70 serves as the loading control ($^{*}p \leq 3.39 \times 10^{-3}$, ANOVA; $n = 5$ independent experiments). ***C–F***, Evaluation of neuronal Plk2, NF-κB, and SPAR kinetics during a PTX (100 μM) time course (0, 3, 7, 12, 24 h) reveals an initial excessive loss of SPAR during Plk2 dominance (3 h; ***C***, ***E***, ***F***), followed by NF-κB activation (***D***) and subsequent partial recovery of SPAR levels (***E***, ***F***). ***F***, Representative Plk2, SPAR, and GAPDH (loading control) immunoblot of hippocampal lysates during PTX time course (quantified in ***C***, ***E***). Plots of NF-κB luciferase reporter assay (***D***) and immunoblot quantification for Plk2 (***C***) and SPAR (***E***) in the same neurons from DIV21 dissociated hippocampal cultures ($^{*}p \leq 0.035$, $^{\#}p = 0.012$; $n \geq 3$ independent experiments). All error bars indicate SEM. ***G***, Summary diagram for the function of the NF-κB transcription factor as an integral feedback sensor in the homeostatic response to chronic elevated activity. Activity-dependent induction of Plk is sufficient to mediate both SPAR protein degradation as well as activation of NF-κB with resulting delayed feedback through NF-κB-dependent upregulation of SPAR expression. These countervailing forces act to tune the outcome of the homeostatic synaptic response, as is revealed by the much more drastic loss of dendritic spine number, size, synaptic receptor content, and function in NF-κB-deficient neurons. Importantly, in mature neurons, these changes do not occur with NF-κB loss under basal conditions, but only in NF-κB-deficient neurons undergoing a homeostatic response to elevated synaptic activity.

with the reduction of SPAR protein following PTX exposure (24 h) that is significantly greater in neurons that are deficient for NF-κB (Fig. 7*A*,*B*). Together, these findings are consistent with an action of NF-κB in opposing Plks at the level of SPAR regulation to dampen response overshooting and establish an end point for homeostatic synaptic responses (Fig. 7*G*, summary diagram).

Discussion

Homeostasis in biological systems is characteristically achieved by employing multiple dynamic compensatory mechanisms that act in antagonizing fashion to reach or fine-tune equilibrium responses. Here we describe the first report of a regulatory feedback mechanism operating during homeostatic synaptic plasticity to prevent excessive loss of synaptic function following chronic elevated activity and to govern the end point of synaptic response. Investigations of homeostatic synaptic plasticity have revealed its importance in the capacity of neuronal networks to maintain stable function over a lifetime, but how precise homeostatic adjustments without excessive or insufficient responses might be achieved and the molecular mechanisms responsible for determining end points of homeostatic responses have remained outstanding issues (Turrigiano, 2008). Our results demonstrate how, in at least one homeostatic pathway, NF-κB functions as an integral feedback sensor (Fig. 7*G*, summary diagram) activated during homeostasis to prevent overshooting and to provide a counterforce to balance Plks in determining the end point of synaptic activity. Features of dendritic spine and synapse number, size, and strength can ultimately impact not only the function of neuronal networks, but also the viability of individual neurons (Segal, 2010). Given the potential benefits that accrue from fine control of homeostatic synaptic plasticity, it is likely that additional mechanisms of checks and balances will be discovered.

We show that the single activity-dependent event of Plk induction is sufficient to mediate both SPAR protein degradation as well as activation of NF-κB. NF-κB activation results in feedback that opposes Plk at the level of SPAR, through NF-κB-dependent SPAR expression. These counterforces act to tune the outcome of the homeostatic synaptic response, as is revealed by the much more drastic loss of dendritic spine number, size, synaptic receptor levels, and function in NF-κB-deficient neurons. Importantly, in mature neurons, synapse changes are not observed with NF-κB loss under basal conditions, but only in NF-κB-deficient neurons undergoing a homeostatic response to chronic elevated synaptic activity.

These studies provide the first evidence of a transcription factor required for appropriate regulation of the homeostatic response. NF-κB transcription factors and components of the canonical NF-κB activation pathway are critically required in many forms of mammalian synaptic plasticity and cognitive performance, including multiple assays of learning and memory (Meffert et al., 2003; Kaltschmidt et al., 2006;

O'Mahony et al., 2006; O'Riordan et al., 2006; Ahn et al., 2008; Russo et al., 2009; Boersma et al., 2011; Christoffel et al., 2011; Schmeisser et al., 2012). At a cellular level, NF-κB (Boersma et al., 2011) and IKK (Russo et al., 2009; Schmeisser et al., 2012) have been shown previously to regulate the development of dendritic spines and synapses. Our results show a physiological role for NF-κB in governing the neuronal homeostatic response to elevated activity that may contribute to the molecular basis of the requirement for NF-κB in excitatory synapse and cognitive function. While NF-κB transcription factors have yet to be implicated in other forms of homeostatic plasticity, it has been reported that global synaptic scaling in response to reduced postsynaptic activity is dependent upon transcription (Ibata et al., 2008). Interestingly, a key molecule postulated to be involved in widespread homeostatic responses to reduced activity, the soluble factor TNFα (Stellwagen and Malenka, 2006), is well known as a classic mediator in the NF-κB pathway that both activates and subsequently is a gene target of NF-κB (Israël et al., 1989; Osborn et al., 1989; Drouet et al., 1991). A potential role for NF-κB in other forms of homeostatic plasticity, including those involving TNFα, remains to be determined.

The induction of Plk expression by heightened neuronal activity was shown previously to lead to SPAR phosphorylation and to target the SPAR protein for degradation through the ubiquitin–proteasome system (Pak and Sheng, 2003; Ang et al., 2008). Our results indicate that SPAR, which stabilizes and promotes mature spines and excitatory synaptic function, is also transcriptionally regulated in an NF-κB-dependent manner both *in vitro* and *in vivo*. The impact of NF-κB-mediated SPAR upregulation in opposing degradation to determine SPAR levels is unmasked by experiments showing that Plk-mediated SPAR loss is more than doubled in NF-κB-deficient compared to wild-type neurons (Fig. 5*A*). A time course of SPAR levels indicates that while loss of SPAR initially predominates following induction of Plk2 by chronic activity, a subsequent recovery of SPAR levels follows concurrent Plk-mediated activation of the NF-κB transcription factor (Fig. 7*C–F*). Exogenous SPAR expression fully rescued the effects of p65 deficiency on measured homeostatic responses to prolonged excitation; however, it remains possible that additional NF-κB-dependent genes also contribute to opposing a homeostatic decline in excitatory synaptic function.

Recent work indicates that Plk2 is induced and regulates synaptic function over a broad range of neuronal activity levels, although its effects may be most profound following episodes of prolonged neuronal excitation (Kauselmann et al., 1999; Lee et al., 2011). Our finding of dose-dependent activation of NF-κB by Plk2 raises the possibility that the integral feedback loop we describe (Fig. 7*G*) might function to equilibrate neuronal excitation in a variety of contexts and add further depth to the understanding of feedback mechanisms regulating neuronal excitation by implicating SPAR as a prolonged-activity responsive gene. NF-κB is a preformed transcription factor that is primarily held latent in the cytoplasm of mature neurons, poised for rapid activation following degradation of the IκB inhibitor. Our data show that both Plk2 and Plk3 are capable of activating neuronal NF-κB through this canonical pathway. While Plk2 appears to be the critical Plk induced and required for homeostatic responses to elevated activity (Seeburg and Sheng, 2008; Seeburg et al., 2008; Lee et al., 2011), Plk3 is responsive to growth factor stimulation, and its specific function in brain and the physiological significance of interaction with the NF-κB pathway are not yet known.

The timing of events inherent to the integral feedback loop we describe is also of potential physiological significance. While the dual kinase-dependent effects of induced Plk2 on both NF-κB activation and SPAR degradation occur on a roughly similar time course, a time delay is necessarily imposed for subsequent opposing effects of activated NF-κB on SPAR levels, which are transcription dependent (Fig. 6). Evaluation of Plk2, NF-κB, and SPAR kinetics during the homeostatic response is consistent with this expected delay, revealing initial excessive loss of SPAR during Plk2 dominance, followed by NF-κB activation and subsequent gain of SPAR levels from earlier time points (Fig. 7). Integral feedback loops are a biological approach used to solve demands for stability and fine-tuning in diverse physiological settings. These results begin to address the molecular gaps in our understanding of feedback mechanisms regulating homeostatic responses and underscore similarities with other long-lasting forms of plasticity that share a requirement for changes in gene expression.

References

Ahn HJ, Hernandez CM, Levenson JM, Lubin FD, Liou HC, Sweatt JD (2008) c-Rel, an NF-kappaB family transcription factor, is required for hippocampal long-term synaptic plasticity and memory formation. Learn Mem 15:539–549. CrossRef Medline

Ang XL, Seeburg DP, Sheng M, Harper JW (2008) Regulation of postsynaptic RapGAP SPAR by Polo-like kinase 2 and the SCFbeta-TRCP ubiquitin ligase in hippocampal neurons. J Biol Chem 283:29424–29432. CrossRef Medline

Boersma MC, Dresselhaus EC, De Biase LM, Mihalas AB, Bergles DE, Meffert MK (2011) A requirement for nuclear factor-kappaB in developmental and plasticity-associated synaptogenesis. J Neurosci 31:5414–5425. CrossRef Medline

Burrone J, O'Byrne M, Murthy VN (2002) Multiple forms of synaptic plasticity triggered by selective suppression of activity in individual neurons. Nature 420:414–418. CrossRef Medline

Chakraborty T, Chowdhury D, Keyes A, Jani A, Subrahmanyam R, Ivanova I, Sen R (2007) Repeat organization and epigenetic regulation of the DH-Cmu domain of the immunoglobulin heavy-chain gene locus. Molecular Cell 27:842–850. CrossRef Medline

Chowdhury D, Sen R (2001) Stepwise activation of the immunoglobulin mu heavy chain gene locus. EMBO J 20:6394–6403. CrossRef Medline

Christoffel DJ, Golden SA, Dumitriu D, Robison AJ, Janssen WG, Ahn HF, Krishnan V, Reyes CM, Han MH, Ables JL, Eisch AJ, Dietz DM, Ferguson D, Neve RL, Greengard P, Kim Y, Morrison JH, Russo SJ (2011) IkappaB kinase regulates social defeat stress-induced synaptic and behavioral plasticity. J Neurosci 31:314–321. CrossRef Medline

Drouet C, Shakhov AN, Jongeneel CV (1991) Enhancers and transcription factors controlling the inducibility of the tumor necrosis factor-alpha promoter in primary macrophages. J Immunol 147:1694–1700. Medline

Evers DM, Matta JA, Hoe HS, Zarkowsky D, Lee SH, Isaac JT, Pak DT (2010) Plk2 attachment to NSF induces homeostatic removal of GluA2 during chronic overexcitation. Nat Neurosci 13:1199–1207. CrossRef Medline

Freudenthal R, Romano A (2000) Participation of Rel/NF-kappaB transcription factors in long-term memory in the crab Chasmagnathus. Brain Res 855:274–281. CrossRef Medline

Ibata K, Sun Q, Turrigiano GG (2008) Rapid synaptic scaling induced by changes in postsynaptic firing. Neuron 57:819–826. CrossRef Medline

Israël A, Le Bail O, Hatat D, Piette J, Kieran M, Logeat F, Wallach D, Fellous M, Kourilsky P (1989) TNF stimulates expression of mouse MHC class I genes by inducing an NF kappa B-like enhancer binding activity which displaces constitutive factors. EMBO J 8:3793–3800. Medline

Kaltschmidt B, Ndiaye D, Korte M, Pothion S, Arbibe L, Prüllage M, Pfeiffer J, Lindecke A, Staiger V, Israël A, Kaltschmidt C, Mémet S (2006) NF-kappaB regulates spatial memory formation and synaptic plasticity through protein kinase A/CREB signaling. Mol Cell Biol 26:2936–2946. CrossRef Medline

Kauselmann G, Weiler M, Wulff P, Jessberger S, Konietzko U, Scafidi J, Staubli U, Bereiter-Hahn J, Strebhardt K, Kuhl D (1999) The polo-like protein kinases Fnk and Snk associate with a Ca(2+)- and integrin-binding protein and are regulated dynamically with synaptic plasticity. EMBO J 18:5528–5539. CrossRef Medline

Lee KJ, Lee Y, Rozeboom A, Lee JY, Udagawa N, Hoe HS, Pak DT (2011)

Requirement for Plk2 in orchestrated ras and rap signaling, homeostatic structural plasticity, and memory. Neuron 69:957–973. CrossRef Medline

Li Z, Niu J, Uwagawa T, Peng B, Chiao PJ (2005) Function of polo-like kinase 3 in NF-kappaB-mediated proapoptotic response. J Biol Chem 280:16843–16850. CrossRef Medline

Lin DT, Makino Y, Sharma K, Hayashi T, Neve R, Takamiya K, Huganir RL (2009) Regulation of AMPA receptor extrasynaptic insertion by 4.1N, phosphorylation and palmitoylation. Nat Neurosci 12:879–887. CrossRef Medline

Meffert MK, Chang JM, Wiltgen BJ, Fanselow MS, Baltimore D (2003) NF-kappa B functions in synaptic signaling and behavior. Nat Neurosci 6:1072–1078. CrossRef Medline

Nimchinsky EA, Sabatini BL, Svoboda K (2002) Structure and function of dendritic spines. Annu Rev Physiol 64:313–353. CrossRef Medline

O'Brien RJ, Kamboj S, Ehlers MD, Rosen KR, Fischbach GD, Huganir RL (1998) Activity-dependent modulation of synaptic AMPA receptor accumulation. Neuron 21:1067–1078. CrossRef Medline

O'Mahony A, Raber J, Montano M, Foehr E, Han V, Lu SM, Kwon H, LeFevour A, Chakraborty-Sett S, Greene WC (2006) NF-kappaB/Rel regulates inhibitory and excitatory neuronal function and synaptic plasticity. Mol Cell Biol 26:7283–7298. CrossRef Medline

O'Riordan KJ, Huang IC, Pizzi M, Spano P, Boroni F, Egli R, Desai P, Fitch O, Malone L, Ahn HJ, Liou HC, Sweatt JD, Levenson JM (2006) Regulation of nuclear factor kappaB in the hippocampus by group I metabotropic glutamate receptors. J Neurosci 26:4870–4879. CrossRef Medline

Osborn L, Kunkel S, Nabel GJ (1989) Tumor necrosis factor alpha and interleukin 1 stimulate the human immunodeficiency virus enhancer by activation of the nuclear factor kappa B. Proc Natl Acad Sci U S A 86:2336–2340. CrossRef Medline

Pak DT, Sheng M (2003) Targeted protein degradation and synapse remodeling by an inducible protein kinase. Science 302:1368–1373. CrossRef Medline

Pak DT, Yang S, Rudolph-Correia S, Kim E, Sheng M (2001) Regulation of dendritic spine morphology by SPAR, a PSD-95-associated RapGAP. Neuron 31:289–303. CrossRef Medline

Papa M, Segal M (1996) Morphological plasticity in dendritic spines of cultured hippocampal neurons. Neuroscience 71:1005–1011. CrossRef Medline

Passini MA, Wolfe JH (2001) Widespread gene delivery and structure-specific patterns of expression in the brain after intraventricular injections of neonatal mice with an adeno-associated virus vector. J Virol 75:12382–12392. CrossRef Medline

Pomerantz JL, Denny EM, Baltimore D (2002) CARD11 mediates factor-specific activation of NF-kappaB by the T cell receptor complex. EMBO J 21:5184–5194. CrossRef Medline

Russo SJ, Wilkinson MB, Mazei-Robison MS, Dietz DM, Maze I, Krishnan V, Renthal W, Graham A, Birnbaum SG, Green TA, Robison B, Lesselyong A, Perrotti LI, Bolaños CA, Kumar A, Clark MS, Neumaier JF, Neve RL, Bhakar AL, Barker PA, et al (2009) Nuclear factor kappa B signaling regulates neuronal morphology and cocaine reward. J Neurosci 29:3529–3537. CrossRef Medline

Schmeisser MJ, Baumann B, Johannsen S, Vindedal GF, Jensen V, Hvalby ØC, Sprengel R, Seither J, Maqbool A, Magnutzki A, Lattke M, Oswald F, Boeckers TM, Wirth T (2012) IkappaB kinase/nuclear factor kappaB-dependent insulin-like growth factor 2 (Igf2) expression regulates synapse formation and spine maturation via Igf2 receptor signaling. J Neurosci 32:5688–5703. CrossRef Medline

Seeburg DP, Sheng M (2008) Activity-induced Polo-like kinase 2 is required for homeostatic plasticity of hippocampal neurons during epileptiform activity. J Neurosci 28:6583–6591. CrossRef Medline

Seeburg DP, Feliu-Mojer M, Gaiottino J, Pak DT, Sheng M (2008) Critical role of CDK5 and Polo-like kinase 2 in homeostatic synaptic plasticity during elevated activity. Neuron 58:571–583. CrossRef Medline

Segal M (2010) Dendritic spines, synaptic plasticity and neuronal survival: activity shapes dendritic spines to enhance neuronal viability. Eur J Neurosci 31:2178–2184. CrossRef Medline

Stellwagen D, Malenka RC (2006) Synaptic scaling mediated by glial TNF-alpha. Nature 440:1054–1059. CrossRef Medline

Sun Q, Turrigiano GG (2011) PSD-95 and PSD-93 play critical but distinct roles in synaptic scaling up and down. J Neurosci 31:6800–6808. CrossRef Medline

Turrigiano GG (2008) The self-tuning neuron: synaptic scaling of excitatory synapses. Cell 135:422–435. CrossRef Medline

Turrigiano GG, Leslie KR, Desai NS, Rutherford LC, Nelson SB (1998) Activity-dependent scaling of quantal amplitude in neocortical neurons. Nature 391:892–896. CrossRef Medline

Wurster AL, Precht P, Pazin MJ (2011) NF-kappaB and BRG1 bind a distal regulatory element in the IL-3/GM-CSF locus. Mol Immunol 48:2178–2188. CrossRef Medline

Yu Z, Cheng G, Wen X, Wu GD, Lee WT, Pleasure D (2002) Tumor necrosis factor alpha increases neuronal vulnerability to excitotoxic necrosis by inducing expression of the AMPA-glutamate receptor subunit GluR1 via an acid sphingomyelinase- and NF-kappaB-dependent mechanism. Neurobiol Dis 11:199–213. CrossRef Medline

Zhu JJ, Qin Y, Zhao M, Van Aelst L, Malinow R (2002) Ras and Rap control AMPA receptor trafficking during synaptic plasticity. Cell 110:443–455. CrossRef Medline

Zhu Y, Pak D, Qin Y, McCormack SG, Kim MJ, Baumgart JP, Velamoor V, Auberson YP, Osten P, van Aelst L, Sheng M, Zhu JJ (2005) Rap2-JNK removes synaptic AMPA receptors during depotentiation. Neuron 46:905–916. CrossRef Medline